

Article

Analysis of the Sum Minimization Possibilities of Heat Exchanger Core Masses in Internal Combustion Engine Cooling Systems

Yuryi Moshentsev ¹, Oleksiy Gogorenko ¹, Olha Dvirna ² and Andrzej Kubit ^{3,*}

¹ Department of Internal Combustion Engines, Installations and Technical Operation, Admiral Makarov National University of Shipbuilding, Heroiv Ukraine Ave. 9, 54007 Mykolaiv, Ukraine; yurii.moshentsev@gmail.com (Y.M.); oleksiy.gogorenko@gmail.com (O.G.)

² Department of Engineering Sciences, Faculty of Marine Engineering, Gdynia Maritime University, 81-87 Morska St., 81-225 Gdynia, Poland; o.dvirna@wm.umg.edu.pl

³ Department of Manufacturing and Production Engineering, Rzeszow University of Technology, al. Powst. Warszawy 8, 35-959 Rzeszow, Poland

* Correspondence: akubit@prz.edu.pl

Abstract: Rational designs for cooling systems (CS) of internal combustion engines are formulated in the form of a series of circulation circuits. The engine is integrated into a circuit with the highest and unregulated flow of internal circuit coolant (ICC). All heat exchangers are placed in circulation circuits with relatively reduced and adjustable ICC flow rates. While the circuits are usually interconnected, they can also be designed to operate independently. This CS scheme enables the achievement of the minimum possible value of the sum of masses of exchanger cores, denoted as M_{Σ} . The reduction in M_{Σ} is achieved through the regulation of ICC flow in a closed circulation loop involving two heat exchangers. The variations in M_{Σ} based on the circuit parameters have been thoroughly investigated. The reduction in M_{Σ} can also be applicable to more intricate systems. A decrease in M_{Σ} , under identical initial CS parameters, may occur in different magnitudes, depending on the specific features of the CS scheme and the operating conditions of the heat exchangers within it. Cooling systems, constructed with the same initial parameters and comprising multiple circulation circuits that meet all criteria for rational design, may exhibit diverse configurations. Examples of such systems are explored, and the minimum values of M_{Σ} are calculated for each. It has been determined that the disparity in the minimum values of M_{Σ} for such systems, while maintaining equal efficiency, can exceed 30%. The selection of the optimal CS scheme is contingent not only on achieving the minimum possible value of M_{Σ} but also on various other factors.

Keywords: central cooler; charge air cooler; cooling system; diesel engine; heat transfer surface; oil cooler



Citation: Moshentsev, Y.; Gogorenko, O.; Dvirna, O.; Kubit, A. Analysis of the Sum Minimization Possibilities of the Heat Exchanger Core Masses in Internal Combustion Engine Cooling Systems. *Appl. Sci.* **2024**, *14*, 314. <https://doi.org/10.3390/app14010314>

Academic Editor: Adrian Irimescu

Received: 3 November 2023

Revised: 20 December 2023

Accepted: 28 December 2023

Published: 29 December 2023



Copyright: © 2023 by the authors. Licensee MDPI, Basel, Switzerland. This article is an open access article distributed under the terms and conditions of the Creative Commons Attribution (CC BY) license (<https://creativecommons.org/licenses/by/4.0/>).

1. Introduction

The motivation for this work is to demonstrate the potential reduction in M_{Σ} in different cooling system schemes by regulating ICC flow rates in circulation circuits. To achieve this objective, ICC flow rates can be regulated in both simple and more complex cooling system configurations. However, variations exist in achieving the minimum M_{Σ} for different cooling system schemes, necessitating an exploration of the features influencing M_{Σ} reduction in various schemes and the reasons for these differences. Modern cooling systems for internal combustion engines are currently implemented through various circulation circuits [1]. The reduction in the total mass of the cores is achieved by leveraging the effect of regulating the flow rate of the ICC in a closed circuit of two heat exchangers [2]. It is noteworthy that, in all works known to us, the focus is on the maximum reduction in the temperature of the coolant downstream of the cooler rather than a decrease in the total mass of the heat exchanger cores, denoted as M_{Σ} [3].

The foundational aspects of the problem are discussed in [4,5], where the focus is on maximizing the reduction of the cooled coolant temperature. The problem is addressed using numerical methods in the context of the simplest circulation circuit. Works such as [6–9] delve into the design possibilities of cooling systems in the form of circulation circuits. While acknowledging the potential for rationalizing cooling systems by regulating ICC flow through heat exchangers, these works lack clear recommendations on the choice of ICC expenditures. Similar observations apply to [10–13].

In [14], the regulation of ICC consumption through the branches of a rational cooling system scheme is explored to reduce M_{Σ} . However, the article does not analyze the possibilities and consequences of reducing M_{Σ} in various specially designed systems with such regulation. In article [15], the authors optimize the cooling system of a marine diesel engine by regulating pump performance while keeping the system design unchanged but open to improvement. Article [16] addresses the enhancement of a cooling system by regulating ICC consumption based on the main engine mode, suggesting the replacement of traditional mechanically driven pumps with electrically driven pumps.

Fundamentally different cooling systems are also under consideration. A comprehensive review of modern adsorption refrigeration systems is provided in [17,18]. However, these systems are characterized by significant dimensions, making their practical use challenging. A substantial portion of the work is dedicated to examining the impact of cooling system operation on engine parameters. Inadequate cooling conditions can result in engine overheating, incomplete combustion, and poor environmental and economic performance [19,20]. Ineffectual cooling also amplifies the cost of consumables [21,22]. In general, phenomena associated with improper cooling conditions contribute to an increase in the concentration of harmful substances in exhaust gases, particularly NOx emissions, power loss, and excessive wear, ultimately leading to a reduction in service life [23,24]. Reducing the service life of machines is detrimental to the environment.

Therefore, any effort aimed at enhancing engine efficiency through effective cooling is crucial, as it results in a reduction in COx emissions [25,26]. Many studies have explored the potential of modifying cooling systems to decrease engine exhaust emissions [27–29]. Additionally, numerous numerical analyses have been conducted to optimize heat distribution in engines, with the goal of minimizing pollutant emissions and reducing fuel consumption [30–32].

Part of this field of study is dedicated to the selection of ICC type. In this article, the authors focus on considering fresh water as an ICC, a choice that facilitates the comparison of cooling systems under equal conditions. However, there is potential for further enhancing cooling system parameters through the use of Nan fluids [33–35]. Notably, [36] suggests that cooling system parameters experience significant improvement when utilizing liquids containing graphene oxide, created based on a combination of ethylene glycol and water. Additionally, [37], a study by Hossen and Sakib, involves numerical simulations of a cooling system, demonstrating that the use of Nan fluids with various compositions notably enhances heat transfer conditions in the cooling system.

For a closed circulation loop consisting of two heat exchangers and two pumps (the simplest cooling system scheme), there are significant variations in M_{Σ} when using optimal and non-optimal ICC flow rates. Similar substantial differences in the values of M_{Σ} are observed in more complex cooling systems, even under identical external conditions, system efficiency, and engine parameters. These disparities are inherent, and it is imperative to identify and elucidate their underlying causes.

The reduction in M_{Σ} stands out as one of the primary key parameters that determine the competitiveness of a cooling system. In principle, the potential for reducing M_{Σ} is evident when the charge air cooling temperature is fixed. However, the task of minimizing M_{Σ} has not yet been explicitly defined or considered as a primary objective, despite its significance. This aspect merits further exploration and attention in the context of cooling system design.

2. Materials and Methods

To analytically address the problem, it is essential to examine a closed system of equations that characterizes the movement of coolant flows and heat flows within the cooling system. However, solving this closed system of equations for the desired quantity (in this case, M_{Σ}), even for the simplest cooling system scheme, results in complex and non-differentiable expressions. Therefore, numerical calculations become necessary. The authors conducted calculations for both the simplest cooling systems with various parameters and more complex systems characteristic of modern internal combustion engines. In the direct calculations of the cooling system, the following parameters were established and determined.

The following were determined: the efficiency of all heat exchangers of the system; the flow rates of coolants through all heat exchangers; all unknown temperatures of coolants; and the masses of the heat exchange elements (cores) of every heat exchanger and of all exchangers of the system, M_i and M_{Σ} .

The following parameters were specified: sea water inlet temperature (T_{ww1}), air temperature behind the compressor (T_1), temperatures of water and oil behind the engine (T_{wm2} , T_{om2}), air temperature in the engine receiver (T_s), fresh water flow through the engine (G_{wm} , equivalent to the flow through the fresh water pump), sea water flow through the pump (G_{ww}), oil flow through the pump (G_m), and charge air flow (G_c). The system was designed to remove strictly defined heat flow values into water, oil, and hydraulic fluid (specified as Q_e , Q_m , and Q_h , respectively). The main (stereotypical) parameters of the designs of all heat exchangers and the efficiency level in utilizing the masses of their cores (represented by coefficients k_{gi}) were also established.

To expedite the design process and ensure the requisite accuracy, all elements of the system design need to be integrated into a unified mathematical model, often referred to as a calculation complex. This complex should incorporate both direct and feedback connections between interacting elements.

When calculating systems, the following assumptions were made:

- The heat transfer process in the design mode is steady.
- Heat losses in the sections of pipelines connecting the heat exchangers are insignificant.
- The ambient temperature is the same for all elements of the cooling system.
- The oil used in the engine system has properties that are practically no different from those specified in the standard for grade M-14W2 (interstate standard 12337-84) [38].

System calculations were performed taking into account the conditions of unambiguity. The basis for direct thermal calculation of the circuit is a system of equations consisting of:

- Heat balance equations for all heat exchangers and the entire cooling system;
- Equations of heat flows in the system;
- Heat balance equations at mixing points of coolant flows;
- Mass balance equations at mixing points of coolant flows;
- Efficiency equations for all heat exchangers;
- Relationship equations between the efficiency of all heat exchangers and their NTU;
- Expressions of the relationship between NTU and the masses of the cores of all heat exchangers.

When working with a specific system of equations, a unique solution can be obtained if the number of equations is equal to the number of unknowns.

For example, in the scheme presented in Figure 1, it is necessary to determine the values of 21 unknowns based on the original system of 19 equations.

Obviously, to achieve an unambiguous solution, it is necessary to additionally specify the values of two unknowns, and the remaining unknowns can then be calculated based on the system of equations. Any two unknowns can be chosen to be set, and it is logical to designate the values of ICC flow rates through the oil cooler and charge air cooler. Moreover, the real regulation of the cooling system will be carried out precisely by adjusting these flow rates. However, the mathematical solution of the problem in this case will be challenging.

It is most convenient to assign temperature values to the ICC behind the oil cooler and charge air cooler, denoted as t_{wo2} and t_{wc2} . This approach simplifies the problem’s solution considerably. The quantities t_{wo2} and t_{wc2} are uniquely related to the ICC flow rates through these heat exchangers; accordingly, optimizing the system becomes more convenient by setting various possible values for these temperatures. As a result, the curves $M_{\Sigma} = f(t_{wo2})$ and $M_{\Sigma} = f(t_{wc2})$ were obtained. To regulate ICC, it is not difficult to obtain similar dependences on ICC flow rates.

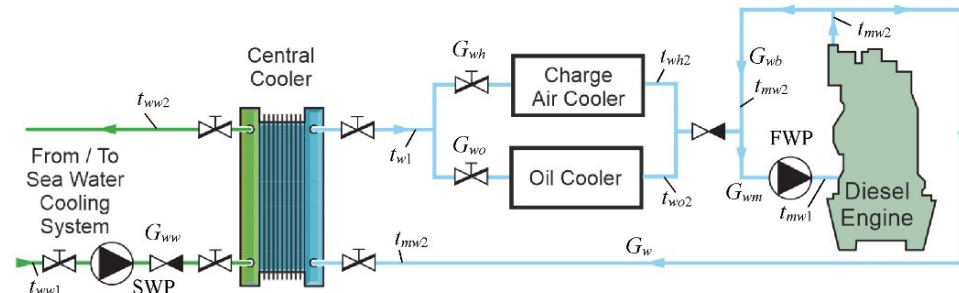


Figure 1. Scheme of the cooling system type A.

For the calculated cooling systems, each curve was plotted at a constant (and rational) value of other specified temperatures. During the initial construction of curves, rational (and constant) values of other temperatures (except for the one changed to construct the curve) were approximated, and then refined based on previously constructed ones. The ultimate value of the minimum parameter, M_{Σ} , was achieved with the same (within the possible error) value of this parameter for all curves. Essentially, this approach outlines one of the methods to obtain an extremum using the coordinate descent method.

3. Results and Discussion

The first system to be studied was the simplest cooling system, as depicted in Figure 2.

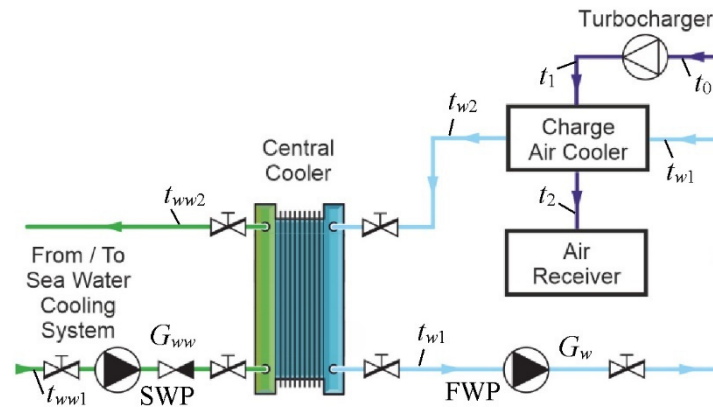


Figure 2. Scheme of the simplest closed cooling system.

A similar scheme was previously studied for a slightly different purpose in [4,5]. In this context, dependencies are derived for such a scheme to observe how M_{Σ} changes when regulating the consumption of ICC (Figure 3).

When constructing graphs and conducting further analysis, the parameter η_0 is utilized, representing the efficiency of the cooling system for cooling the charge air

$$\eta_0 = \frac{T_1 - T_s}{T_1 - T_{ww1}},$$

where $T_{1,s}$ —temperatures of charge air in front of the compressor and in the engine receiver, K; T_{ww1} —temperature of external circuit coolant (ECC) in front of the cooler, K.

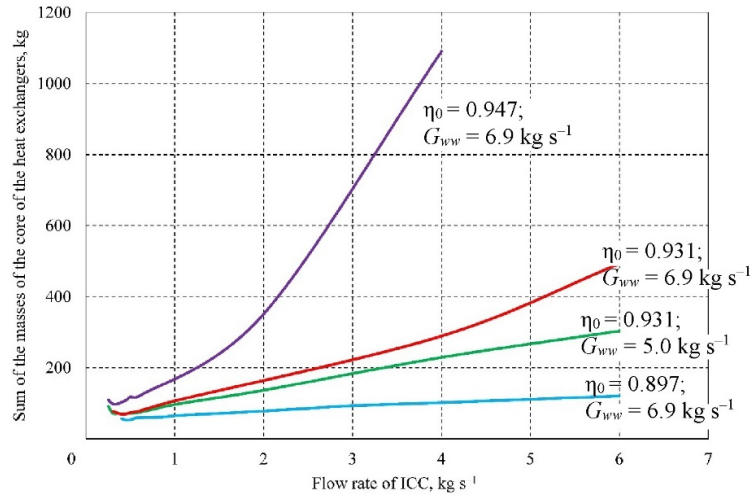


Figure 3. Dependences of M_{Σ} for different constant values of η_0 and for different values of G_{ww} on the ICC flow rate G_w in the circuit.

The dependencies were plotted for various values of η_0 and different external circuit coolant costs— G_{ww} . The calculations were conducted for one of the modern medium-speed marine engines, and the necessary parameters for these calculations are provided in Table 1.

Table 1. The main parameters of the engine for which the simplest cooling systems were calculated.

Designation	Items	Values
N_e	Engine output (kW)	1000
n	Engine speed (rpm)	500
p_c	Boost pressure (bar)	2.0
G_c	Charge air flow (kg s^{-1})	0.9
p_0	Ambient pressure (bar)	1.0
t_0	Ambient temperature ($^{\circ}\text{C}$)	40.0
t_1	Air temperature after compressor ($^{\circ}\text{C}$)	181.35
t_{ww1}	Sea water temperature in front of the pump ($^{\circ}\text{C}$)	30.0
t_2	Air temperature in the receiver ($^{\circ}\text{C}$)	35.0

In greater detail, the initial section of one of the curves in Figure 3 is illustrated in Figure 4. Here, it can be observed that it exhibits a characteristic bend, influencing the value of M_{Σ} at low ICC flow rates.

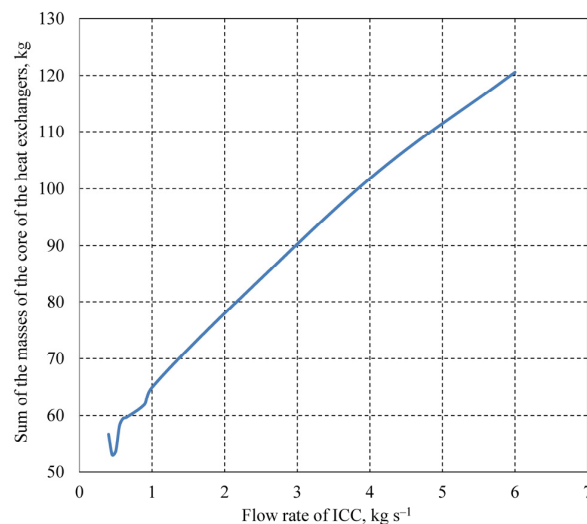


Figure 4. Example of the calculated graph of the dependence of M_{Σ} on the flow rate of the ICC G_w .

Analysis of the dependencies in Figures 3 and 4 allows us to note the following features.

1. In a closed simple circuit, there is a significant variation in M_{Σ} depending on the flow of ICC through the heat exchangers.
2. As G_w increases from values close to zero, the value of M_{Σ} first decreases (Figure 4), and then consistently increases monotonically for any constant values of η_0 .
3. For all possible η_0 , the minimum values of M_{Σ} are achieved at relatively low values of the ICC flow rate G_w .
4. The values of M_{Σ} decrease as G_w decreases and increase as G_w increases.
5. The increase in M_{Σ} depending on G_w varies for different values of η_0 ; as η_0 as η_0 increases, the growth of M_{Σ} becomes more pronounced.
6. The ratios M_{Σ} for two different η_0 increase as the values of η_0 and the absolute value of M_{Σ} rise—they can exceed 1000% in the region of large values of G_w within practical ranges of G_w and η_0 .

Next, an analysis was conducted on the position of the minimum points of M_{Σ} for the simplest cooling system, depending on the ratio of the energy capacities of the coolants in the charge air cooler S_c .

$$S_c = W / W_w,$$

where $W = G_H \cdot c_{pH}$; $W_w = G_w \cdot c_{pw}$ —the energy capacities being referred to are those of the charge air and internal circuit coolant, respectively; c_{pH} —the isobaric heat capacity of air; c_{pw} —the heat capacity of internal circuit coolant.

The position of the minimum point M_{Σ} for various values of η_0 and G_{ww} was determined by analyzing the initial sections of the curves $M_{\Sigma} = f(S_c)$. Examples of such regions are shown in Figures 5 and 6.

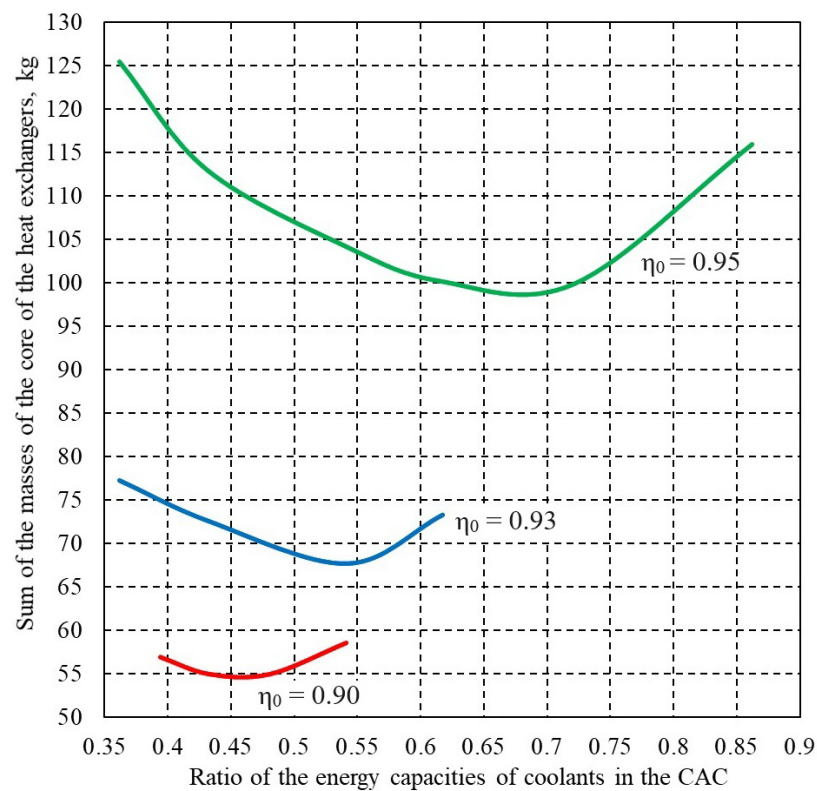


Figure 5. The initial sections of the curves $M_{\Sigma} = f(S_c)$ at different η_0 and constant consumption of ECC, $G_{ww} = 5.5 \text{ kg s}^{-1}$.

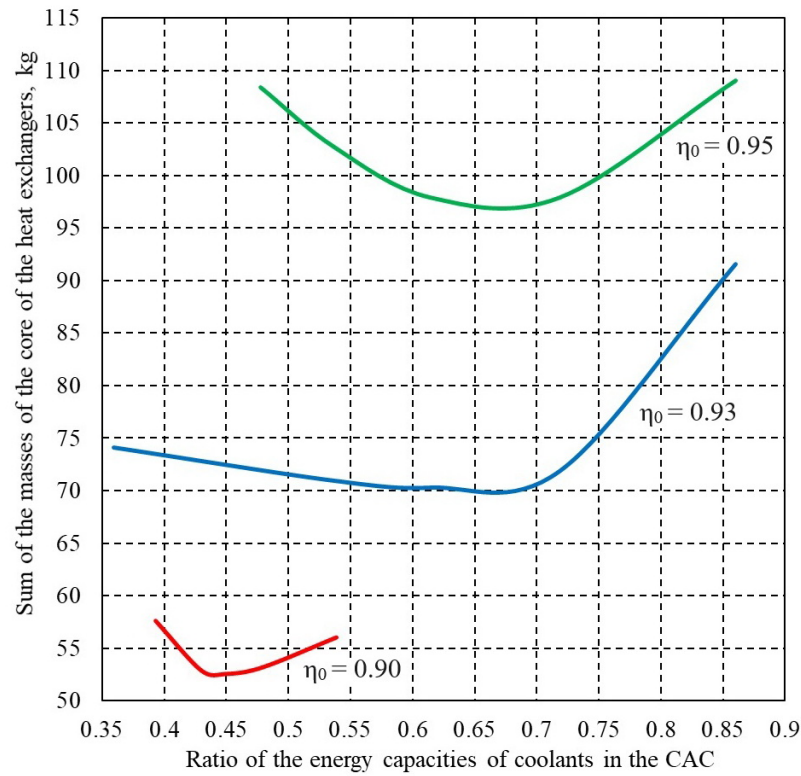


Figure 6. The initial sections of the curves $M_{\Sigma} = f(S_c)$ at different η_0 and a constant consumption of ECC, $G_{ww} = 6.9 \text{ kg s}^{-1}$.

The position of the minimum points allows for some deviations associated with the shape of the curves and the specifics of the systems and heat exchangers under consideration. Based on the comprehensive analysis, it is evident that the value of S_c , corresponding to the minimum value of M_{Σ} , practically depends only on η_0 and can be reasonably approximated by the expression

$$S_c = 6.0263\eta_0 - 5.0311.$$

It has also been established that for the range $\eta_0 = 0.90 \dots 0.95$ with rational S_c (corresponding to the minimum value of M_{Σ}), the charge air cooler efficiency value is approximately constant and corresponds to t_0

$$\eta_c \approx 0.97.$$

With an irrational value of S_c , the efficiency of the charge air cooler, η_c , significantly affects M_{Σ} . The value of M_{Σ} decreases monotonically with increasing η_c . If in the simplest cooling system, the flow rate of ICC, G_w , is increased to the possible limit (up to the consumption through the engine), then the value of M_{Σ} will increase. The value of M_c can either increase or decrease.

For example, for an engine whose parameters correspond to Table 1, at $\eta_0 = 0.9$ and $G_w = 4.0 \text{ kg s}^{-1}$ (optimal S_c), the value of $M_{\Sigma} = 281.5 \text{ kg}$, $M_c = 126 \text{ kg}$ at $\eta_c = 0.97$.

At $\eta_0 = 0.9$, $G_w = 22.2 \text{ kg s}^{-1}$ (maximum G_w), then $M_{\Sigma} = 416.9 \text{ kg}$, $M_c = 136.2 \text{ kg}$, $\eta_c = 0.99$.

At $\eta_0 = 0.953$ (for optimal S_c), the value is $M_{\Sigma} = 394 \text{ kg}$, $M_c = 211 \text{ kg}$ (optimum $G_w = 2.0 \text{ kg s}^{-1}$, $\eta_c = 0.97$).

At $\eta_0 = 0.953$, $G_w = 22.2 \text{ kg s}^{-1}$ (maximum G_w), the value is $M_{\Sigma} = 1201 \text{ kg}$, $M_c = 135 \text{ kg}$ ($\eta_c = 0.99$).

As can be seen from the provided data, the variation in M_{Σ} is contingent on η_0 and exhibits a substantial increase with its growth, aligning with one of the conclusions drawn.

The efficiency of the second heat exchanger, η_w , contingent on η_0 , and for the same range of η_0 , can be approximated by the expression

$$\eta_w = 0.2941\eta_0 + 0.667.$$

The accuracy of cooling system calculations and potential errors primarily depend on the precision of heat exchanger calculations. This work employs widely accepted methods for calculating heat exchangers, and system calculations are carried out based on established mathematical and thermal engineering principles. The objectives of this work preclude the possibility of experimental verification for all the presented material. Nevertheless, the key results of experimental checks related to the accuracy of heat exchanger calculations and the validity of calculation methods for the cooling system can be provided. These checks were conducted to validate the calculations of the simplest cooling system, serving as the foundation for all subsequent calculations. Specifically, the elements of boundary conditions for heat exchangers were scrutinized, and the correctness of the chosen methods for cooling system calculations was verified. The primary outcomes are presented in Tables 2–4.

Checks were conducted for different objects under various conditions, reflecting the diverse characteristics of both the objects and the feasibility of experimental verification for fairly large full-scale objects. The results from the tables indicate that the checks yielded quite satisfactory outcomes, providing a solid basis to consider all the information presented here as reliable.

The patterns identified for the simplest circuit can be extrapolated to more complex cooling system circuits if they incorporate the simplest circuit without modifications. However, there exist numerous cooling system schemes that utilize the concept of regulating the flow of ICC through heat exchangers, yet cool the coolants under conditions that do not align with those discussed above.

Table 2. Estimation of errors for charge air cooler.

Designation	Items	Values			Note
		I	II	III	
t_2	Air temperature after charge air cooler (°C)	35.81	35.71	34.41	Calculation
		35.70	35.52	34.12	Experiment
Δt_2	Difference air temperature after charge air cooler (°C)	0.11	0.19	0.29	
Δp	Air resistance (bar)	0.0157	0.0107	0.0095	Calculation
		0.0150	0.0101	0.0090	Experiment
δ	Difference air resistance	0.045	0.058	0.049	
η_c	Charge air cooler efficiency	0.94	0.95	0.97	
G_c	Charge air flow (kg s ⁻¹)	0.9	0.7	0.6	Experiment
p_1	Boost pressure (bar)	2.0	1.7	1.5	Experiment

Table 3. Estimation of errors for central cooler.

Designation	Items	Calculation	Experiment
G_w	ICC flow rate by fresh water pump (kg s ⁻¹)	0.32	
G_{ww}	ECC flow rate by sea water pump (kg s ⁻¹)	5.50	
t_{w1}	Inlet ICC water temperature (°C)	91.46	91.40
t_{w2}	Outlet ICC water temperature (°C)	30.02	30.30
t_{ww1}	Temperature of ECC in front of the cooler (°C)	30.00	30.00
Δp_w	Resistance by ICC (bar)	0.00268	0.00305
Δp_{ww}	Resistance by ECC (bar)	0.00137	0.00123
δ_w	Error Δp_w	0.139	
δ_{ww}	Error Δp_{ww}	0.105	
η_w	Central cooler efficiency	0.999	0.995

Table 4. Estimation of errors for cooling system.

Designation	Items	Calculation	Experiment	Measurement Error
t_{ww1}	Temperature of ECC in front of the cooler (°C)	30.00	30.00	± 0.30
t_1	Air temperature after compressor (°C)	125.78	126.20	± 0.70
t_2	Air temperature after charge air cooler (°C)	35.00	37.20	± 0.75
t_{w1}	Charge air cooler inlet water temperature (°C)	30.22	31.30	± 0.30
t_{w2}	Charge air cooler outlet water temperature (°C)	91.46	91.40	± 0.75
p_0	Ambient pressure (bar)	1.0	1.013	$\delta p = 0.028$
p_1	Boost pressure (bar)	2.0	1.956	
G_c	Charge air flow (kg s ⁻¹)	0.9	0.9 *	$\delta G = 0.020 \dots 0.025$
G_{ww}	ECC flow rate by sea water pump (kg s ⁻¹)	5.5	5.5 *	
G_w	ICC flow rate by fresh water pump (kg s ⁻¹)	0.32	0.32 *	
η_c	Charge air cooler efficiency	0.950	0.934	$\delta^{**} = 0.030 \dots 0.037$
η_w	Central cooler efficiency	0.996	0.994	
η_0	Cooling system efficiency	0.950	0.954	

* Measured with specified error. ** For the entire measurement range.

Below, we explore more complex systems in which the charge air cooler is integrated into the overall circuit, and another where it operates in a separate circuit. These systems are designed for an engine with parameters outlined in Table 5. Both circuits and their heat exchangers are state-of-the-art. The selected schemes are evaluated at $\eta_0 = 0.9$.

Table 5. The results of the system calculations for various loads and ambient temperatures.

Designation	Items	Values
N_e	Engine output (kW)	2950
N	Engine speed (rpm)	1000
p_c	Boost pressure (bar)	2.94
G_c	Charge air flow (kg s ⁻¹)	5.30
p_0	Ambient pressure (bar)	1.0
t_0	Ambient temperature (°C)	40.0
t_1	Air temperature before compressor (°C)	181.35
t_{ww1}	Sea water temperature in front of the pump (°C)	30.0
t_2	Air temperature in the receiver (°C)	48.0
t_{m1}	Engine oil temperature behind the engine (°C)	90.0
t_{h1}	Hydraulic fluid temperature behind the system (°C)	90.0
G_w	ICC flow rate by fresh water pump (kg s ⁻¹)	22.2
G_{ww}	ECC flow rate by sea water pump (kg s ⁻¹)	22.2
G_m	Oil flow rate (kg s ⁻¹)	26.6
G_h	Hydraulic fluid flow rate (kg s ⁻¹)	4.0
Q_e	Heat flow from engine cylinders (kW)	1058.0
Q_m	Heat flow from oil (kW)	531.4
Q_h	Heat flow from hydraulics (kW)	40.0

Since the definition of M_Σ is linked to specific designs of heat exchangers and types of heat exchange surfaces, the numerical values of the masses of the heat exchanger cores cannot be considered absolute, even for engines with similar parameters. However, the obtained mass values are convenient for comparing different options.

The first of the cooling systems with a complex circuit is the type A cooling system (Figure 1). For this system, the highest value of the minimum M_Σ was obtained. The circuit is designed with a charge air cooling circuit integrated into the overall system circuit.

The hot ICC is discharged from the full-flow circuit of the cooling system after the engine has cooled. ICC from the full-flow circuit enters the cooler for cooling, after which it bifurcates into parallel flows to cool the charge air in the charge air cooler and the oil in the oil cooler. Subsequently, the ICC streams are combined, and the merged stream, with a temperature T_{wb} and flow rate G_{wb} , enters the full-flow cooling system loop before the fresh water pump. When combining the ICC flows after the engine and after the heat exchangers, the ICC temperature decreases to the required value T_{mw1} in front of the engine. The results of minimizing M_{Σ} are presented in Table 6. The operational efficiency of each heat exchanger in the cooling system is characterized by the dimensionless criterion I_x [39].

$$I_x = \frac{Q_i}{\Delta T_i W_{ix}},$$

where Q_i —the heat flow through the heat exchanger, W; ΔT_i —temperature difference between heat carriers (average logarithmic temperature difference), K; W_{ix} —energy intensity of the cold coolant, W/K.

Table 6. Main parameters of the cooling systems at the minimum M_{Σ} .

Designation	Items	Cooling System Type				
		A	B	C	D	E
		Values				
η_H	Charge air cooler efficiency	0.995	0.993	0.968	0.967	0.944
S_H	Energy-capacity ratio	0.225	0.30	0.389	0.374	0.403
M_H	Charge air cooler core mass	178.3	194.9	137.7	157.6	115.7
I_{xH}	Dimensionless criterion for charge air cooler	1504	1.498	–	–	–
η_w	Central cooler efficiency	0.808	0.735	–	–	–
S_w	Energy-capacity ratio	0.62	0.663	–	–	–
M_w	Central cooler core mass	1011.4	756.0	–	–	–
I_{xw}	Dimensionless criterion for central cooler	1.947	1.476	–	–	–
η_{wc1}	Central cooler No. 1 efficiency	–	–	0.864	0.867	0.907
S_{wc1}	Energy-capacity ratio	–	–	0.153	0.159	0.119
M_{wc1}	Central cooler No. 1 core mass	–	–	153.4	165.6	151.2
η_{wc2}	Central cooler No. 2 efficiency	–	–	0.851	0.965	0.806
S_{wc2}	Energy-capacity ratio	–	–	0.329	0.193	0.147
M_{wc2}	Central cooler No. 2 core mass	–	–	378.5	347.8	353.7
η_{wc3}	Central cooler No. 3 efficiency	–	–	–	0.547	–
S_{wc3}	Energy-capacity ratio	–	–	–	0.139	–
M_{wc3}	Central cooler No. 3 core mass	–	–	–	48.2	–
η_g	Hydraulic fluid cooler efficiency	–	–	0.555	0.717	0.43
S_g	Energy-capacity ratio	–	–	0.268	0.157	0.549
M_g	Hydraulic fluid cooler core mass	–	–	38.9	39.2	25.7
η_{oc}	Oil cooler efficiency	0.365	0.565	0.555	0.717	0.486
S_{oc}	Energy-capacity ratio	0.624	0.399	0.536	0.314	0.549
M_{oc}	Oil cooler core mass	251.7	312.7	454.7	392.0	362.5
I_{xoc}	Dimensionless criterion for oil cooler	0.52	0.617	–	–	–
M_{Σ}	Total mass of cores heat exchangers	1441.4	1263.6	1163.2	1150.4	1008.8
I_{xcs}	Dimensionless criterion for cooling system	3.972	3.591	–	–	–

When comparing a number of systems, it is necessary to consider their differences and account for changes within the systems. Simultaneously, this applies to both heat exchangers and the overall system

$$I_{xci} = I_{xpi} \frac{W_{xcc}}{W_{xec}}$$

where I_{xci} —adjusted criterion; I_{xpi} —the initial value of the criterion; W_{xcc} —the energy capacity of the cold coolant for the compared system, W/K; W_{xec} —the energy intensity of the cold coolant for the reference system, W/K.

As M_{Σ} increases in the system, the I_x criterion also increases, and vice versa. Therefore, when designing both systems and heat exchangers, one should aim to minimize the numerical value of the criterion. In this case, all systems will be compared with cooling system type A, considering it as the least favorable among those compared. Type A cooling system is regarded as a reference.

Next, a type B cooling system was studied (Figure 7). In this system, the hot ICC flow is extracted from the full-flow circuit for cooling after the fresh water pump (FWP1), before reaching the engine. The ICC then enters the inlet of the second fresh water pump (FWP2), after which it flows into the central cooler, where it is cooled to temperature t_{w1} .

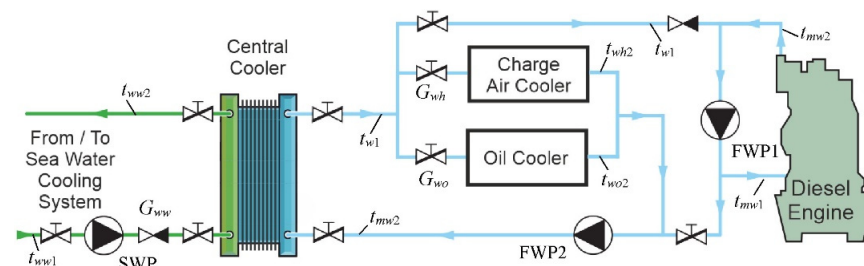


Figure 7. Scheme of the cooling system type B.

Then, it flows to the inlets of the charge air cooler and oil cooler, and after passing through these coolers, the ICC returns to the full-flow circuit. After the coolers, the ICC flows are combined and, at a temperature t_{wt} , they proceed to the inlet of the FWP2 pump. By incorporating a portion of the cooled ICC flow into the full-flow circuit, at the input of FWP1, and mixing it with the flow leaving the engine, the temperature t_{mv1} is maintained in front of the engine. The key parameters of this cooling system and other schemes, at the minimum of M_{Σ} , are presented in Table 6.

As evident from Table 6, for the type B cooling system, the minimum value of M_{Σ} is significantly reduced compared to the previous version. In alignment with the I_{xw} criterion value, the heat exchanger with the largest core mass in this system operates under conditions of a higher temperature difference than the previous scheme. The masses of the charge and oil cooler cores experienced slight increases, but a substantial reduction in M_{Σ} was achieved, as confirmed by the corresponding criterion. In principle, for any cooling system, an increase in the sum of the masses of the heat source cores is accompanied by a decrease in the sum of the masses of the heat sink cores and vice versa. The patterns of growth and reduction in the masses of heat exchanger cores depend on the adopted design of the cooling system.

Comparing the first two cooling systems, the following observations can be made. In the cooling system type A circuit, hotter fuel oil is extracted from the full-flow circuit than in the cooling system type B, but this does not result in an increase in the temperature difference on the central cooler. At first glance, the indicated temperature difference should have increased, but this did not happen. The organization of the previous system imposes certain restrictions on reducing the costs of ICC through heat exchangers. Specifically, it is impossible to achieve the required ICC temperature in front of the engine if its flow through these heat exchangers is too low. This, in turn, limits the increase in temperature difference for the central cooler.

As shown in Table 6, η_c exceeds the value corresponding to the minimum M_{Σ} for the simplest circuit. The value of S_c is very close, and the core mass is greater. This is attributed to the rationalization of other heat exchangers in the circuit. It should be noted that the values of S for the oil cooler and central cooler for the schemes under consideration significantly exceed the values that occur for circuits that do not take advantage of the effect of reducing ICC consumption. As per Table 6, M_{Σ} for the type B system decreased by almost 180 kg compared to the type A system. The primary reduction was achieved by reducing the mass of the central cooler core.

Let us examine a type C cooling system scheme (Figure 8), in which a reduction in M_{Σ} is achieved by increasing the number of central coolers. This offers expanded possibilities for regulating the flow of ICC through heat exchangers (Table 6).

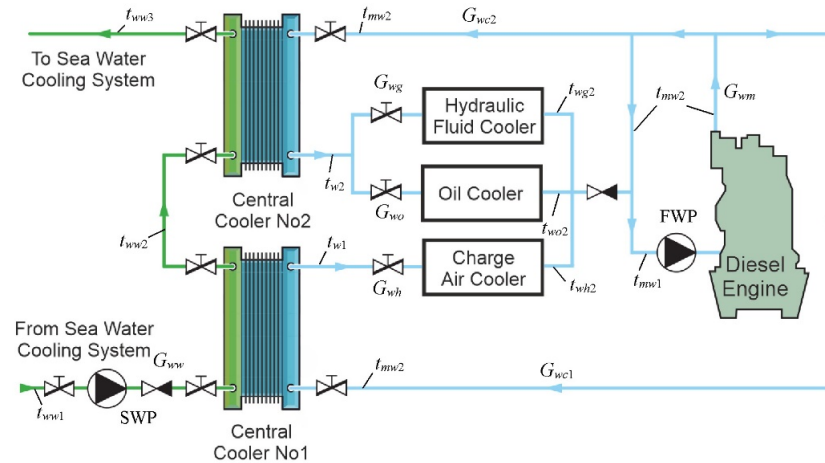


Figure 8. Scheme of cooling system type C.

This and the subsequent systems utilize a hydraulic fluid cooler. The mass of its core is very small, approximately 39 kg. For this reason, the presence of this heat exchanger has no practical impact on the comparison results of the cooling systems. The values of η_{c} , S_c , and M_c here are close to the values established for the simplest circuit. The parameters of the remaining heat exchangers are determined based on the decrease in M_{Σ} . The reduction in M_{Σ} for this system, compared to the previous one, is more than 100 kg. Compared to cooling system type A, it is about 280 kg. A further reduction in M_{Σ} can be achieved through even better possibilities for regulating ICC flow rates through the system heat exchangers. However, for the considered schemes and similar ones, these possibilities are practically exhausted. Increasing or even maintaining the temperature difference for the heaviest heat exchangers is challenging. This can be illustrated by the diagram of the type D cooling system (Figure 9). A central cooler No. 3 is installed here, which should remove part of the heat flow from the engine and expand the possibilities of regulating the flow through other heat exchangers. However, due to the installation of this cooler, the temperature differences in all heat exchangers are reduced, except for the central cooler No. 3, which counteracts a further significant decrease in M_{Σ} (Table 6).

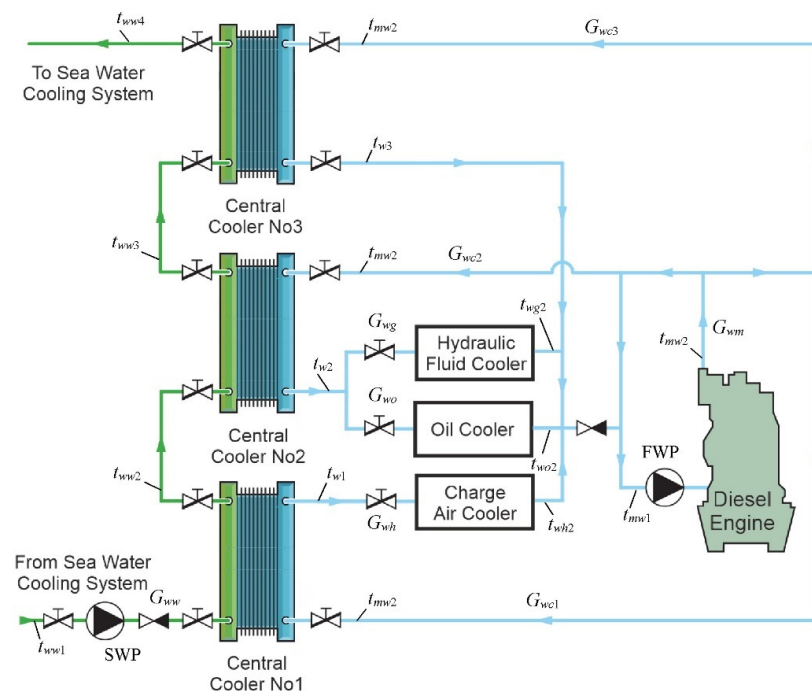


Figure 9. Scheme of cooling system type D.

4. Simultaneous minimization of all masses of the heat exchanger cores M_i in a complex system, when regulating the ICC flow rates to find the minimum M_Σ , does not occur: some M_i increase, others decrease.
5. In various complex low-flow cooling systems, with the same engine parameters, different minimum values of M_Σ are possible. This depends on the conditions of using heat exchangers with the largest M_i in the cooling system: they must be placed in conditions of the greatest efficiency of their operation.
6. For the researched, relatively complex, rational cooling systems, their total core masses M_Σ can be different for the same engine and at the same operating mode. Importantly, this difference turned out to be significant. As can be seen from Table 6, the M_Σ values of the lightest and heaviest of the systems can differ by approximately 35% with the same efficiency of these systems. Other systems occupy intermediate positions.

Author Contributions: Conceptualization, Y.M.; methodology, Y.M. and O.G.; software, O.G. and O.D.; validation, Y.M., O.G., O.D. and A.K.; formal analysis, Y.M. and A.K.; data curation, O.G.; writing—original draft preparation, Y.M.; writing—review and editing, O.G. and A.K.; visualization, O.D.; supervision, O.D. and A.K.; project administration, O.D. All authors have read and agreed to the published version of the manuscript.

Funding: This work was commissioned by the PrJSC Berislavsky Machine-Building Plant (Ukraine) under the contract No. 516.12/010 on scientific and technical cooperation. This research did not receive any specific grant from funding agencies in the public, commercial, or not-for-profit sectors.

Institutional Review Board Statement: Not applicable.

Informed Consent Statement: Not applicable.

Data Availability Statement: The data presented in this study are available on request from the corresponding author upon request. The data are not publicly available due to privacy.

Conflicts of Interest: The authors declare no conflict of interest and that they have no financial and personal relationships with other people or organizations that could inappropriately influence their work, and that there is no professional or other personal interest of any nature or kind in any product, service, and/or company that could be construed as influencing the position presented in, or the review of, the manuscript entitled.

Nomenclature

G	Flow rate (kg s^{-1})
M	Mass (kg)
Q	Heat transfer rate (kW)
t	Temperature ($^{\circ}\text{C}$)
p	Pressure (bar)
Subscripts	
1	Before
2	Behind
c	Charge air
h	Hydraulic fluid
o	Oil
w	Internal circuit coolant
ww	Outer circuit coolant
Σ	Total
Abbreviations	
ECC	External circuit coolant
FWP	Fresh water pump
IC	Internal combustion
ICC	Internal circuit coolant
SWP	Sea water pump

References

1. Ganesh, D.; Nagarajan, G. Homogeneous charge compression ignition (HCCI) combustion of diesel fuel with external mixture formation. *Energy* **2010**, *35*, 148–157. [\[CrossRef\]](#)
2. Deng, X.; Lei, J.; Wen, J.; Wen, Z.; Shen, L. Multi-objective optimization of cooling galleries inside pistons of a diesel engine. *Appl. Therm. Eng.* **2018**, *132*, 441–449. [\[CrossRef\]](#)
3. Brace, C.J.; Hawley, G.; Akehurst, S.; Piddock, M.; Pegg, I. Cooling system improvements—Assessing the effects on emissions and fuel economy. *Proc. Inst. Mech. Eng. Part D J. Automob. Eng.* **2008**, *222*, 579–591. [\[CrossRef\]](#)
4. Kays, W.M.; London, A.L. *Compact Heat Exchangers*; Mc Graw—Hill Book Company: New York, NY, USA, 1964.
5. Eastwood, J.C. Liquid-Coupled Indirect-Transfer Exchanger Application to the Diesel Engine. *J. Eng. Power* **1979**, *101*, 516–523. [\[CrossRef\]](#)
6. Mathur, G.D.; Hara, J.; Iwasaki, M.; Meguriya, Y. *Development of an Innovative Energy Efficient Compact Cooling System “SLIM”*; SAE Technical Papers; SAE International: Warrendale, PA, USA, 2012.
7. Cipollone, R.; Di Battista, D.; Gualtieri, A. A novel engine cooling system with two circuits operating at different temperatures. *Energy Convers. Manag.* **2013**, *75*, 581–592. [\[CrossRef\]](#)
8. *Application & Installation Guide Cooling Systems*; CAT, Caterpillar, BUILT FOR IT: Peoria, IL, USA, 2016.
9. Mollenhauer, K.; Tschoeke, H. *Handbook of Diesel Engines*; Springer: Berlin/Heidelberg, Germany, 2010; pp. 291–338.
10. Nutt, R.A.; Poehlman, R.F. *Cooling System Requirements for Advanced Diesel Engines*; SAE Technical Paper Series 820984; SAE International: Warrendale, PA, USA, 1982.
11. Sekar, R.R. Trends in Diesel Engine Charge Air Cooling. *SAE Trans.* **1982**, *91*, 2102–2113.
12. Daminov, O.O.; Khushnaev, O.A.; Yangibaev, A.I.; Kucharenok, G.M. Improving the performance indicators of diesel engines by enhancing the cooling system. *Tech. Sci. Innov.* **2020**, *2020*, 63–68. [\[CrossRef\]](#)
13. Moshentsev, Y.; Gogorenko, O.; Dvirna, O. Rational Liquid Cooling Systems of Internal Combustion Engines. *Adv. Sci. Technol. Res. J.* **2022**, *16*, 158–169. [\[CrossRef\]](#)
14. Zhang, B.; Zhang, P.; Zeng, F. Multiobjective optimization of the cooling system of a marine diesel engine. *Energy Sci. Eng.* **2021**, *9*, 1887–1907. [\[CrossRef\]](#)
15. Śliwiński, K.; Szramowiat, M. Development of cooling systems for internal combustion engines in the light of the requirements of modern drive systems. *IOP Conf. Ser. Mater. Sci. Eng.* **2018**, *421*, 042078. [\[CrossRef\]](#)
16. Hamdy, M.; Askalany, A.A.; Harby, K.; Kora, N. An overview on adsorption cooling systems powered by waste heat from internal combustion engine. *Renew. Sustain. Energy Rev.* **2015**, *51*, 1223–1234. [\[CrossRef\]](#)
17. Vittorini, D.; Bartolomeo, D.; Battista, D.; Cipollone, R. Charge Air Subcooling in a Diesel Engine via Refrigeration Unit—Effects on the Turbocharger Equilibrium. *Energy Procedia* **2018**, *148*, 822–829. [\[CrossRef\]](#)
18. Demonstrator, L.L.R.; Ricci, D.; Battista, F. Transcritical Behavior of Methane in the Cooling Jacket of a Liquid-Oxygen/Liquid Methane Rocket-Engine Demonstrator. *Energies* **2022**, *15*, 4190.
19. Gumus, M. Reducing cold-start emission from internal combustion engines by means of thermal energy storage system. *Appl. Therm. Eng.* **2009**, *29*, 652–660. [\[CrossRef\]](#)
20. Sirsikar, S.; Mehta, V.; Chafekar, K.; Sonawane, G.; Dandekar, Y. Review Paper of Engine Cooling System. *Int. Res. J. Eng. Technol.* **2020**, *7*, 4538–4541.
21. Wagner, J.R.; Srinivasan, V.; Dawson, D.M.; Marotta, E.E. *Smart Thermostat and Coolant Pump Control for Engine Thermal Management Systems*; SAE International: Warrendale, PA, USA, 2003.
22. Bai, S.; Han, J.; Liu, M.; Qin, S.; Wang, G.; Li, G.-X. Experimental investigation of exhaust thermal management on NO_x emissions of heavy-duty diesel engine under the world Harmonized transient cycle (WHTC). *Appl. Therm. Eng.* **2018**, *142*, 421–432. [\[CrossRef\]](#)
23. Tao, X.; Wagner, J.R. An Engine Thermal Management System Design for Military Ground Vehicle—Simultaneous Fan, Pump and Valve Control. *SAE Int. J. Passeng. Cars—Electron. Electr. Syst.* **2016**, *9*, 243–254. [\[CrossRef\]](#)
24. Liu, H.; Wen, M.; Yang, H.; Yue, Z.; Yao, M. A Review of Thermal Management System and Control Strategy for Automotive Engines. *J. Energy Eng.* **2021**, *147*, 03121001. [\[CrossRef\]](#)
25. Zhou, B.; Lan, X.D.; Xu, X.H.; Liang, X.G. Numerical model and control strategies for the advanced thermal management system of diesel engine. *Appl. Therm. Eng.* **2015**, *82*, 368–379. [\[CrossRef\]](#)
26. Kaleli, A.; Kaltakkiran, G.; Dumlu, A.; Ayten, K.K. Design and control of intelligent cooling system for IC engine. In Proceedings of the 2017 International Conference on Engineering and Technology (ICET), Antalya, Turkey, 21–23 August 2017.
27. Khanjani, K.; Deng, J.; Ordys, A. *Controlling Variable Coolant Temperature in Internal Combustion Engines and Its Effects on Fuel Consumption*; SAE International: Warrendale, PA, USA, 2014.
28. Mohamed, M.; Shedid, M.H.; El-Demerdash, M.S.; Fatouh, M. Performance of Electronically Controlled Automotive Engine Cooling System Using PID and LQR Control Techniques. *IOSR J. Mech. Civ. Eng.* **2018**, *15*, 42–51.
29. Cipollone, R.; Di Battista, D.; Contaldi, G.; Murgia, S.; Mauriello, M. Development of a sliding vane Rotary pump for engine cooling. *Energy Procedia* **2015**, *81*, 775–783. [\[CrossRef\]](#)
30. Banjac, T.; Wurzenberger, J.C.; Kutrašnik, T. Assessment of engine thermal management through advanced system engineering modeling. *Adv. Eng. Softw.* **2014**, *71*, 19–33. [\[CrossRef\]](#)

31. Roy, B.K.; Sharma, N.K. Control strategies for advanced thermal management system in IC engine. *Int. J. Eng. Res. Technol.* **2013**, *6*, 225–231.
32. Jadeja, K.M.; Bumataria, R.; Chavda, N. Nanofluid as a coolant in internal combustion engine—A review. *Int. J. Ambient. Energy* **2023**, *44*, 363–380. [[CrossRef](#)]
33. Tarodiya, R.; Sarkar, J. Cooling of an internal combustion engine using nanofluids: A review. In Proceedings of the National Conference on “Advances in Thermal Engineering”, Indore, India, 14 October 2011; pp. 75–82.
34. Che Sidik, N.A.; Witri Mohd Yazid, M.N.A.; Mamat, R. Recent advancement of nanofluids in engine cooling system. *Renew. Sustain. Energy Rev.* **2017**, *75*, 137–144. [[CrossRef](#)]
35. Prasanna Shankara, R.; Banapurmath, N.R.; D’Souza, A.; Sajjan, A.M.; Ayachit, N.H.; Yunus Khan, T.M.; Badruddin, I.A.; Kamangar, S. An insight into the performance of radiator system using ethylene glycol-water based graphene oxide nanofluids. *Alex. Eng. J.* **2022**, *61*, 5155–5167. [[CrossRef](#)]
36. Hossen, A.; Sakib, N. Numerical Analysis on Heat Transfer with Nanofluid in an Automotive Radiator Numerical Analysis on Heat Transfer with Nanofluid in an Automotive Radiator. In Proceedings of the International Conference on Mechanical, Industrial and Energy Engineering 2020, Khulna, Bangladesh, 19–21 December 2020.
37. Ap, N.-S.; Tarquis, M. *Innovative Engine Cooling Systems Comparison*; SAE Technical Papers; SAE International: Warrendale, PA, USA, 2005.
38. Motor Oils for Diesel Engines. Specifications. Available online: https://dnaop.com/html/71289/doc-%CE%93OCT_12337-84 (accessed on 26 December 2023).
39. Moshentsev, U.; Gogorenko, A. Generating high efficiency cooling systems for internal combustion engines. *Her. Enginebuilding J.* **2017**, 25–31. Available online: <http://vd.zntu.edu.ua/article/view/114053> (accessed on 26 December 2023).

Disclaimer/Publisher’s Note: The statements, opinions and data contained in all publications are solely those of the individual author(s) and contributor(s) and not of MDPI and/or the editor(s). MDPI and/or the editor(s) disclaim responsibility for any injury to people or property resulting from any ideas, methods, instructions or products referred to in the content.